Closed-Form Expressions for the Current Density on the Ground Plane of a Microstrip Line, with Application to Ground Plane Loss

Christopher L. Holloway and Edward F. Kuester

***Abstract*—In this paper closed-form expressions for the current density on the ground plane of a microstrip line are derived. The derivation is based on a quasistatic Green's function approach. These expressions are compared to both experimental and numerical values, and excellent agreement is demonstrated. The loss on a ground plane for a microstrip structure is calculated using these expressions, and comparisons with results from Wheeler's incremental inductance rule are made.**

I. Introduction

Microstrip lines are used in numerous electronic devices and products ranging from feeding networks in MIMIC components to signal traces on printed circuit boards. The current distribution on the ground plane of the microstrip line can be important for design considerations. For example, knowledge of ground plane current distribution can aid in determining the amount of coupling between adjacent printed circuit traces fabricated on a common ground plane (see [18]), or can aid in determining how wide a truncated ground plane might need to be to ensure that edge effects are acceptably low. Knowing this current distribution can also aid in determining the loss due to finite conductivity of the ground plane (see Section III).

Numerical techniques can be used to obtain the current on the ground plane. These techniques are capable of high accuracy, but are computationally intensive and hence do not lend themselves to simple design procedures. The current on the ground plane can be derived from an integration of the current on the strip with a Green's function. In this paper two different approximate expressions for the current distribution on the strip are used. The first is a very crude constant approximation for the strip current, whereas the second is the more accurate Kobayashi distribution.

This paper is organized as follows: After the introduction, the Section II presents derivations of the ground plane current distributions for different strip current approximations. Section III illustrates how the loss due to the ground plane can be calculated, and compares this to results obtained from Wheeler's incremental inductance rule. In Section IV, other applications of these closed-form expressions are discussed.

II. Derivation of a Closed Form Expression for the Ground Plane current on a Microstrip Line

If the H fields for the microstrip line (Fig. 1) are known then the current density on the ground plane can be found by

$$J_{GP}(x) = \bar{a}_n \times \bar{H}\big|_{y=-h}. \tag{1}$$

In general, all three vector components of current may exist. However, in planar circuits the J_z component of the current is often the dominant component, as shown in [14] and [15]. Schumacher [15] shows that up to $12\,GHz$ (for $\frac{w}{h} = .98$), the ratio $\frac{|J_x|_{max}}{|J_z|_{max}} \leq 0.1$. When this ratio is squared, the result is only 1.0% of the total power loss. Kobayashi [14] also shows that even as high as 20 GHz (for $\frac{w}{h} = 10$ and smaller), the ratio $\frac{|J_x|_{max}}{|J_z|_{max}} \leq 0.15$. Little generality is lost by considering this quasi-TEM case, and so only the z component of the current, and thus the x component of the H-field, is needed.

Manuscript received November 1, 1993; revised September 23, 1994.
C. L. Holloway is with the Institute for Telecommunication Sciences, U.S. Department of Commerce, Boulder, CO 80303 USA.
E. F. Kuester is with the Department of Electrical and Computer Engineering, University of Colorado, Boulder, CO 80309-0425 USA.
IEEE Log Number 9410340

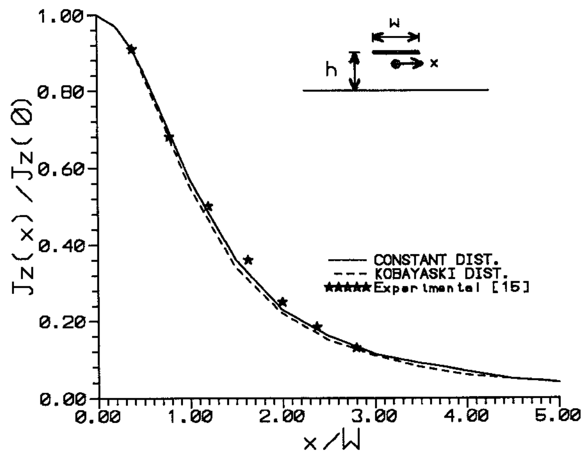

Fig. 1. Results for the normalized current density for a microstrip for $w = 0.62$ mm and $h = 0.635$ mm, where x is the distance measured from the center of the strip. Also shown here are the experimental results obtained from Schumacher [15]. The solid curve corresponds to a constant strip current, the dashed curve corresponds to the Kobayaski distributions, and the stars corresponds to Schumacher's experimental results.

The x component of the H-fields can be obtained from the $z$component of the magnetic vector potential ($\bar{A}$), where A_z can be found from a quasistatic Green's function approach (for details see [12]). Leaving out the details, it can be shown that the current density on the ground plane reduces to

$$J_{GP}(x) = -\frac{h}{\pi}\int_{-w/2}^{w/2} J_z(x')\frac{dx'}{[(x-x')^2+h^2]} \tag{2}$$

where w is the width of the strip and h is the height of the strip above the ground plane (see Fig. 1).

If the current density on the strip is known then the current density on the ground plane is determined from (2). In this paper two different approximate expressions for the current distribution on the strip are used to determine $J_{GP}(x)$. The first is a crude constant approximation for J_z, whereas the second is the more accurate Kobayashi distribution.

A. Calculation for J_{GP} With a Constant Current Distribution on the Strip

In this section the ground plane current is calculated by assuming that the current on the strip takes on the form: $J_z = \frac{I}{w}$, where I is the total current on the strip.

Upon substitution into (2), the current density on the ground plane reduces to the simple closed form expression

$$J_{GP}(x) = -\frac{I}{w\pi}\left[\tan^{-1}\left(\frac{w-2x}{2h}\right) + \tan^{-1}\left(\frac{w+2x}{2h}\right)\right]. \tag{3}$$

Fig. 1 shows the results for the normalized current density $(\frac{J_{GP}(x)}{J_{GP}(0)})$ for a microstrip for $\frac{w}{h} = 0.98$. Also shown on this figure are the experimental results obtained by Schumacher [15] for $w = 0.62$ mm and $h = 0.635$ mm. This experiment was performed

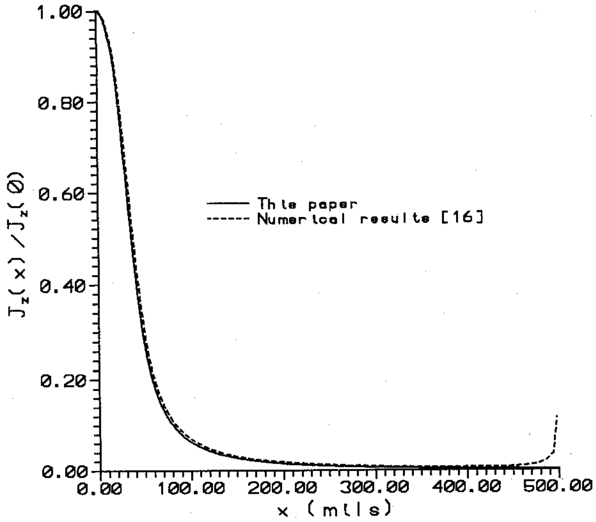

Fig. 2. Comparison of the ground plane current density calculated from (3) to numerical values [16] with $h = 20$ mils and $w = 60$ mils. The numerical values where calculated for a frequency of 3 GHz. The solid curve corresponds to (3) and the dashed curve corresponds to the numerical values.

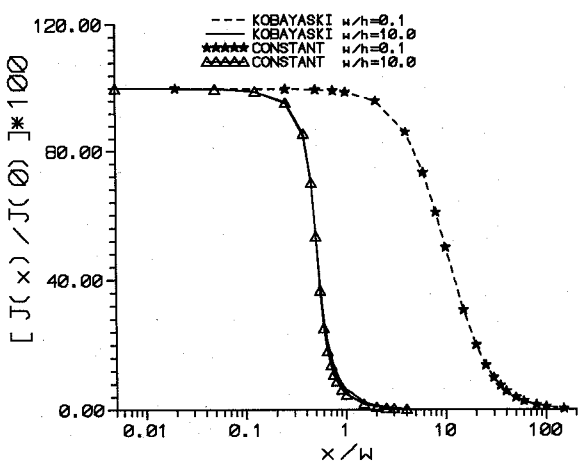

Fig. 3. Comparison of the ground plane current density for both the constant strip current distribution (3) and for the Kobayashi strip current distribution (4) for $h = 100$ μm. The solid curve correspond to $\frac{w}{h} = 10$ and the dashed curve corresponds to $\frac{w}{h} = 0.1$.

with the microstrip operating at a frequency of 18GHz. For these values of w and h, the quasi-TEM approximation is well justified, and even with this crude approximation to the strip currents, the correlation between these two results is excellent. Fig. 2 shows a comparison for the normalized current density from (3) to numerical results obtained from a hybrid finite-element/MOM code [16]. This comparison once again shows excellent agreement. The numerical results were calculated for a frequency of 3 GHz with $\frac{w}{h} = 3$, $h = 20$ mils and for a ground plane of width 50 h. Notice that the numerical results reproduce the edge behavior of the truncated ground plane. This effect is discussed later.

Fig. 3 shows results for the normalized current density for various values of $\frac{w}{h}$. The curve shows that for very narrow microstrips the ground plane current spreads out far from the strip edges. However, for wide microstrips the current is concentrated under the strip.

B. Calculation for J_{GP} with the Kobayashi current distribution on the strip

Presently, the Kobayashi distribution [14] is accepted as being the most accurate closed-form approximation to the current density on the strip. This distribution will now be used to determine $J_{GP}(x)$. With the Kobayashi distribution, the current on the ground plane reduces to the following:

$$J_{GP}(x) = -\frac{I}{C}\left\{\frac{(1-K)}{\pi}\left[\tan^{-1}\left(\frac{w-2x}{2h}\right)+\tan^{-1}\left(\frac{w+2x}{2h}\right)\right] - \frac{KA}{\sqrt{2}}\left[\frac{\left[(x^2-h^2-A^2)^2+4h^2x^2\right]^{1/2}-(x^2-h^2-A^2)}{\left[(x^2-h^2)^2+4h^2x^2\right]-2A^2x^2+3A^4}\right]^{\frac{1}{2}}\right\} \tag{4}$$

where

$$A = \frac{w}{2} \quad ; \quad K = \frac{10(1-\frac{x_c}{A})\sqrt{A^2-x_c^2}}{A-\sqrt{A^2-x_c^2}}$$

and

$$C = (1-K)w + \frac{\pi K w}{2}.$$

Fig. 1 shows how the results of this equation correlate with Schumacher's experimental values. The plots show how (4) does an excellent job of predicting the ground plane current density. This figure also shows that there is very little difference between (3) (constant current on strip) and (4) (Kobayashi distribution). This point is further demonstrated in Fig. 3. In this figure the ground plane current densities predicted from both (3) and (4) are plotted for different values of $\frac{w}{h}$. This figure shows that there is essentially no difference between the two distributions. Therefore, the simpler of the two expressions in (3) can be used.

III. Calculation of Ground Plane Loss

Characterizing the conductor loss for planar circuits, such as for microstrips or coplanar waveguides (CPW), has been the object of much attention, especially recently [1]–[10]. In recent work [11] and [12], closed-form expressions for the conductor loss for both microstrips and coplanar waveguides (CPW) were derived.

The expression for the attenuation constant of microstrip line given in [11, (117)] is due to the conducting strip only (it does not include ground plane losses), and was shown to be valid for a wide range of strip thickness to skin depth ratios ($\frac{t}{\delta_{sk}}$). In order to compare our predicted loss for a microstrip to experimental data for situations where the ground plane loss may be significant (that is for large $\frac{w}{h}$), the effects of ground plane loss on the attenuation constant needs to be characterized.

Figs. 8 and 9 in [11] illustrate the importance of ground plane loss on the total loss of the structure. In these figures the strip loss calculated from [11, (117)] is compared to experimental data taken from Goldfarb and Platzker [4]. Also shown in these two figures are results for loss when both the strip and ground plane losses are included. As expected, for the narrow strips, there is essentially no difference in the results with or without the ground plane loss. For the wider strip however, the predicted conductor loss correlates very well with the experimental when the ground plane loss is included.

The standard manner of calculating the ground plane loss is based on Wheeler's incremental inductance rule [1], and is of the form

$$\alpha_c = \frac{R_s}{2\mu_o Z_o}\sum_j \frac{\partial L}{\partial n_j}$$

where Z_o is the characteristic impedance, L is the inductance per unit length, $\frac{\partial L}{\partial n_j}$ denotes the derivative of L with respect to the

$$\alpha_{GP} = \frac{R_s}{2Z_o}\left(\frac{1}{w\pi}\right)^2 \int_{-\infty}^{\infty}\left[\tan^{-1}\left(\frac{w-2x}{2h}\right)+\tan^{-1}\left(\frac{w+2x}{2h}\right)\right]^2 dx \tag{6}$$

incremental recession of wall j of the structure in the normal direction, and R_s is the standard Leontovich surface impedance [13].

The attenuation constant computed from Wheeler's rule can be separated into two parts, one part corresponding to the loss on the ground plane, and the second part corresponding to the loss on the strip. For a wide range of applications this expression works well. However, if $\frac{t}{\delta_{sk}}$ is small (where δ_{sk} is the skin depth and t is the thickness of a conductor) or even comparable to 1, then the Wheeler rule breaks down giving very poor results for the loss on the strip. This is due in part to the fact that the Leontovich surface impedance is no longer valid. On the other hand, the part of the expression that corresponds to the loss on the ground plane is still fairly accurate for large skin depths (as long as the thickness of the ground plane is large compared to the skin depth), because the Leontovich surface impedance is still valid. In this paper, we present an alternative approach to the calculation of the ground plane loss which does not require knowledge of L and its dependence on ground plane position, but only on the characteristic impedance of the line and its geometric parameters.

Using a standard wall loss perturbation analysis, it can be shown that the loss in the ground plane is given by

$$\alpha_{GP} = \frac{R_s}{2Z_o I^2} \int_{-\infty}^{\infty} |J_{GP}(x)|^2 \, dx \tag{5}$$

where R_s is the Leontovich surface impedance, Z_o is the characteristic impedance of the microstrip line, I is the total current, and $J_{GP}(x)$ is the current density on a perfectly conducting ground plane. Using (3) for the ground plane current density α_{GP} reduces to (6), shown at the bottom of the previous page. Unfortunately this integral cannot be evaluated in closed form to get an explicit expression for the ground plane loss and must be evaluated numerically.

The ground plane losses predicted by (6) and that obtained from applying Wheeler's rule for a given microstrip structure are shown in Fig. 4 for $f = 2$ GHz and $f = 20$ GHz respectively. This figure shows that both methods predict approximately the same loss for $\frac{w}{h} < 1$. Above this value the curves start to deviate. This deviation is probably traceable to the derivative of L needed in Pucel's formula [2]. Wheeler [17] claims that his formulas for L are accurate to 1%, but this assertion says nothing about the accuracy of derivatives of L and therefore caution must be used when employing values of $\frac{\partial L}{\partial n_j}$ computed in this way. It should be noted that for most applications $\frac{w}{h} < 1$, and for these cases there is essentially no difference in the two methods.

IV. Conclusion

A Green's function approach was used to derive two different expressions for the current on the ground plane of a microstrip line. These expressions have been compared to both experimental and numerical values, and excellent correlation was demonstrated. We have also shown that there is very little difference between the two expressions for the current, and if the current on the ground plane is needed, the simpler of the two expressions (3) can be used without significant loss in accuracy.

Equation (3) was used to calculate the loss due to the ground plane for a microstrip structure, and was shown to agree well with results from Wheeler's rule, especially for $\frac{w}{h} < 1$. Even for $1 < \frac{w}{h} < 10$ the relative discrepancy in α_{GP} does not exceed 10%.

A procedure similar to that given in Section II-A has also been used to determine the ground plane current on a coupled line. The result is, as one might expect, a superposition of terms in the form of (3) due to the different lines. If one is interested in the ground plane loss of a coupled microstrip structure, then such a result could be inserted into (5).

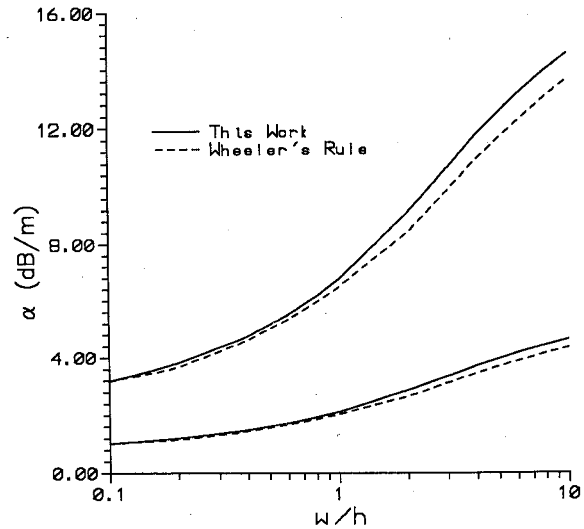

Fig. 4. Comparison for the results from Pucel's formula for the ground plane loss to the results presented here, see (6). These two sets of curve were generated for $h = 100$ μm and for $f = 2$ and 10 GHz, respectively. The solid curves are our results and the dashed curves are the results from Pucel's formula.

Adjacent printed circuit lines fabricated on circuit boards used in electronic products can be investigated with the results presented in this paper. The simple closed form expression for the current density on the ground plane (3) allows one to investigate how the current spreads out from under the strip. The spreading out of the current density on the ground plane influences the coupling between adjacent circuit traces located above a common ground plane, as discussed by Johnson and Graham [18]. Johnson and Graham [18] have a heuristic expression for the ground plane current which they relate to coupling (or crosstalk) between adjacent traces.

This expression can also be used to indicate how close to the edge of a ground plane a microstrip line can be located or how wide a truncated ground plane might need to be. In order for the edge effects to be minimized, the current density close to the edge must be sufficiently small. Equation (3) provides an analytical basis by which to estimate this effect.

This expression was derived assuming that the ground plane was infinitely wide. The current density near the edges of a finite ground plane becomes large and our expression cannot reproduce this. However, as shown in Fig. 2, our expression is correct everywhere except within about 50 mils from the edge for a 1000-mil-wide ground plane. This expression can be used to give an indication of how large a ground plane may be needed such that the current is undisturbed.

References

[1] H. A. Wheeler, "Formulas for the skin effect," *Proc. IRE*, vol. 30, pp. 412–424, 1942.
[2] R. A. Pucel, D. J. Massé, and C. P. Hartwig, "Losses in microstrip," *IEEE Trans. Microwave Theory Tech.*, vol. 12, no. 6, pp. 342–350, 1968.
[3] H. J. Finlay, R. H. Jansen, J. A. Jenkins, and I. G. Eddison, "Accurate characterization and modeling of transmission lines for GaAs MIMIC's," *IEEE Trans. Microwave Theory Tech.*, vol. 36, no. 6, pp. 961–967, 1988.
[4] M. E. Goldfarb and A. Platzker, "Losses in GaAs microstrip," *IEEE Trans. Microwave Theory Tech.*, vol. 38, no. 12, pp. 1957–1963, 1990.
[5] W. Heinrich, "Full-Wave analysis of conductor losses on MIMIC transmission lines," *IEEE Trans. Microwave Theory Tech.*, vol. 38, no. 10, pp. 1468-1472, 1990.
[6] E. Paleczny, D. Kinowski, J. F. Legier, P. Pribetich, and P. Kennis, "Comparison of full wave approaches for determination of microstrip conductor losses for MIMIC applications," *Electron. lett.*, vol. 26, no. 25, pp. 2076–2077, 1990.

[7] L. P. Vakanas, A. C. Cangellaris, and J. L. Prince, "A parametric study of the attenuation constant of lossy microstrip lines," *IEEE Trans. Microwave Theory Tech.*, vol. 38, no. 8, pp. 1136–1139, 1990.
[8] V. V. Nokil'skiy and A. Y. Kozlov, "Electrodynamic analysis of the losses in microstrip line conductors taking their multilayer structure into account," *Telecommun. Radio Eng.*, vol. 41/42, no. 12 pp. 103–108, 1987.
[9] H.-Y. Lee and T. Itoh, "Phenomenological loss equivalence method for planar quasi-TEM transmission lines with a thin normal conductor or superconductor," *IEEE Trans. Microwave Theory Tech.*, vol. 37, no. 12, pp. 1904–1909, 1989.
[10] W. Heinrich, "Mode-Matching approach for superconducting planar transmission lines including finite conductor thickness," *IEEE Microwave and Guided Wave Lett.*, vol. 1, no. 10, pp. 294–296, 1991
[11] C. L. Holloway and E. F. Kuester, "Edge shape effects and quasiclosed form expressions for the conductor loss of microstrip lines," *Radio Sci.*, vol. 29, no. 3, 1994.
[12] C. L. Holloway, "Edge and surface shape effects on conductor loss associated with planar circuits," Electromagnetics Laboratory, Dept. of Electrical and Computer Engineering, Univ. of Colorado, MIMICAD Tech. Rep. no. 12, Appendix G, 1992.
[13] M. A. Leontovich, "Approximate boundary conditions for an electromagnetic field at the surface of a highly conducting body," in *Issledovaniya po Rasprostraneniyu Radiovoln*, pt. 2. Moscow, 1948, pp. 5–12, in Russian; also in —— *Izbrannye Trudy: Teoreticheskaya Fizika.* Moscow: Nauka, 1985, pp. 351–355.
[14] M. Kobayashi, "Longitudinal and transverse current distributions on microstrip and their closed-form expression," *IEEE Trans. Microwave Theory Tech.*, vol. 33, no. 9, pp. 784–788, 1985.
[15] W. Schumacher, "Stromverteilung auf der grundfläche der mikrostrip leitung und deren auswirkung auf die ohmsche leitungsdampfung," *AEÜ*, band 33, pp. 207–212 1979.
[16] M. Labelle and D. Jankovic, Dept. of Electrical and Computer Engineering, Electromagnetics Laboratory, Univ. of Colorado, Boulder, private communication.
[17] H. A. Wheeler, "Transmission-line properties of parallel wide strips by a conformal-mapping approximation," *IEEE Trans. Microwaves Theory Tech.*, vol. 12, no. 3, pp. 280–289, 1964.
[18] H. W. Johnson and M. Graham, *High-Speed Digital Design: A Handbook of Black Magic.* Englewood Cliffs, NJ: Prentice Hall, 1993 pp. 191–192.

Determination of the Eigenfrequencies of a Ferrite-Filled Cylindrical Cavity Resonator Using the Finite Element Method

Gilbert C. Chinn, Larry W. Epp, and Gregory M. Wilkins

***Abstract*—A formulation of the Finite Element Method (FEM) particular to axisymmetric problems containing anisotropic media is compared to an analytic solution. In particular, the resonant frequencies of a longitudinally biased ferrite-filled cylindrical cavity are examined. For comparison, a solution of the characteristic equation for the lossless, ferrite-filled cylindrical waveguide was modified to give the resonant frequencies of the cylindrical cavity. This analytical solution was then used to examine the error in the FEM formulation for the anisotropic case. It is noted that the FEM formulation for anisotropic material presented, based on both node and edge-based elements, is found to be free of spurious solutions.**

Manuscript received January 24, 1994; revised September 8, 1994. This work was supported by the Jet Propulsion Laboratory, California Institute of Technology, under a contract with the National Aeronautics and Space Administration

G C. Chinn and L. W. Epp are with the Jet Propulsion Laboratory, California Institute of Technology, Pasadena, CA 91109 USA.

G. M. Wilkins is with Morgan State University, Baltimore, MD USA.

IEEE Log Number 9410350.

I. Introduction

IT IS NATURAL to extend tangential vector finite elements to not only inhomogeneities, but to the anisotropic case. Specifically, Wang and Ida [1] were able to show that this extension could be free of spurious modes. Their method was based on the use of tetrahedral and hexahedral elements. They noted that for permeability tensors without off-diagonal terms, symmetry could be applied to simplify the analysis. This simplification, however, is not suitable for ferrite-filled cylindrical cavities. For a ferrite-filled cylindrical waveguide, Dillon *et al.* [2] applied periodic boundary conditions to solve for phase constants. This procedure reduces the order of the solution to one-half of the original three dimensional problem.

Another method of reducing computational complexity is detailed here. By applying a Fourier mode expansion to the fields in these azimuthally invariant geometries, simplification is inherent. All modal information is retained, important for the ferrite-filled cavity where the resonant frequencies of the $\pm n$ modes can differ. The FEM analysis is thus effectively reduced to two dimensions.

Axisymmetric geometries of interest in the past included circular waveguides filled with longitudinally biased ferrites. Solutions for the phase constants of these ferrite-filled circular waveguides can be modified for the ferrite-filled cavity. Application of the appropriate boundary conditions then gives a characteristic equation which is solved for the eigenfrequencies. This solution will be outlined, and used as comparison for the FEM analysis.

II. Finite Element Formulation

The tensor characterizing a longitudinally biased ferrite is given by

$$\bar{\mu} = \begin{pmatrix} \mu & -j\mu' & 0 \\ j\mu' & \mu & 0 \\ 0 & 0 & \mu_z \end{pmatrix} \tag{1}$$

where μ, μ', and μ_z are functions of frequency and the DC biasing field for a magnetized ferrite. Because of the axisymmetry of the problem, the weak form of the wave equation is written in terms of electric field components normal and transverse to the ϕ direction using first order triangular nodal elements and first order edge-based finite elements [3]. The field is then expanded as a Fourier sum over the azimuthal variable, ϕ. The basis elements for this expansion are chosen to go as $e^{jn\phi}$. This choice is necessary in order to correctly model the fields within media characterized by (1). Moreover, it also allows the eigenvalues, corresponding to the eigenfrequencies here, to be found independently for each value of n by solving the generalized eigenvalue equation for the cavity

$$[\mathbf{S}]\{a\} = k_o^2[\mathbf{T}]\{a\}. \tag{2}$$

This formalism yields sparse real-symmetric $[\mathbf{S}]$ and $[\mathbf{T}]$ matrices for lossless, Hermitian $\bar{\mu}$ tensors. Consequently, standard mathematical library routines are used to solve the generalized eigenvalue equation.

III. Analytic Characteristic Equation

The analytic characteristic equation for cylindrical ferrite waveguides is due to Kales [4]. In this section, a brief summary of its modification for the particular case of a metallic cavity is presented. The cavity under consideration has a radius of R and a length of L and is filled with a single material described by (1).

Application of the boundary conditions at the ends of the cavity requires the longitudinal electric field component, $\mathbf{E}_z$, and the transverse magnetic field component, $\vec{\mathbf{H}}_t$, to vary as $\cos(\gamma z)$ while $\mathbf{H}_z$